Sensitivity of DDVCS observables to GPDs

Juan Sebastian Alvarado
Mostafa Hoballah - Eric Voutier
IJCLab - Orsay

DIS2024
09/04/2024

GPDs

- At low energy QCD, we need structure functions to describe the nucleon structure.
- **Generalized Parton Distributions** (GPDs) correlate the transverse position and longitudinal momentum of partons in the nucleon.
- They enter the cross-section of exclusive inelastic scattering processes through **Compton Form Factors** (CFFs).

$$\mathcal{F}(\xi, t) \equiv \mathcal{P}\int_{-1}^{1} dx\, F(x, \xi, t)\left(\frac{1}{x-\xi+i\epsilon} \pm \frac{1}{x+\xi+i\epsilon}\right).$$

- For a spin 1/2 particle there are four chiral-even GPDs: $F = H, E, \tilde{H}, \tilde{E}$.

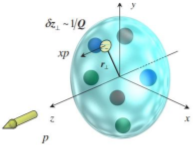

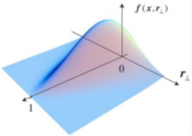

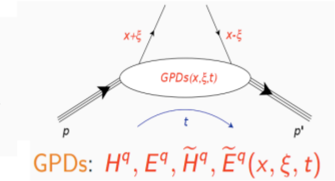

Exclusive leptoproduction reactions

Two golden channels for GPD measurements are **DVCS** and **DDVCS** (See K. Deja, V. Martinez-Fernandez et al. Phys. Rev. D 107.9 (2023), p. 094035.).

$ep \to ep\gamma$

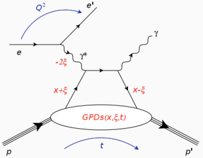

Deeply Virtual Compton Scattering (DVCS)

$$\mathcal{H}(\xi,\xi,t) = \sum_q e_q^2 \Big\{ \mathcal{P} \int_{-1}^{1} dx\, H^q(x,\xi,t) \left[\frac{1}{x-\xi} + \frac{1}{x+\xi} \right] - i\pi \left[H^q(\xi,\xi,t) - H^q(-\xi,\xi,t) \right] \Big\}$$

- **Pros:**
  - Easier to access experimentally.
  - Direct GPD measurement from $\Im$(CFF).
- **Cons:**
  - GPD measurements only at $x = \pm\xi$.

$ep \to epl^- l^+$

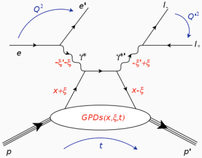

Double DVCS (DDVCS)

$$\mathcal{H}(\xi',\xi,t) = \sum_q e_q^2 \Big\{ \mathcal{P} \int_{-1}^{1} dx\, H^q(x,\xi,t) \left[\frac{1}{x-\xi'} + \frac{1}{x+\xi'} \right] - i\pi \left[H^q(\xi',\xi,t) - H^q(-\xi',\xi,t) \right] \Big\}$$

- **Pros:**
  - GPD measurement at independent $x = \xi'$ and ξ values.
  - Generalizes the results from DVCS and TCS. See Victor's talk on Wednesday!
- **Cons:**
  - Need for a muon detector.
  - Smaller cross section.

DDVCS experimental observables

- We consider a muon pair in the final state, polarized electron/positron beams and a polarized **proton target**.
  - At JLab (12 GeV beam energy):
    - ✓ A muon detection is planned (SoLID collaboration) [1].
    - ✓ A positron beam is planned (PEPPo, Ce^+BAF and JLab positron working group) [2–4].
  - At EIC (140 GeV CoM energy):
    - ✓ Electron and positron beams might be expected [5].
    - ✓ Muon detection might be possible.
- Given the notation $\mathcal{O}_{\text{Beam pol,Target pol}}$, let us define the following observables:
  - Beam Spin Asymmetry (BSA) $A_{LU} = \frac{d^5\sigma_{+U} - d^5\sigma_{-U}}{d^5\sigma_{UU}}$.
  - Target Spin Asymmetry (TSA) $A_{UL} = \frac{d^5\sigma_{U+} - d^5\sigma_{U-}}{d^5\sigma_{UU}}$.
  - Double Spin Asymmetry (DSA) $A_{LL} = \frac{(d^5\sigma_{++} - d^5\sigma_{+-}) - (d^5\sigma_{-+} - d^5\sigma_{--})}{d^5\sigma_{UU}}$.
  - Unpolarized Beam Charge Spin Asymmetry (BCA) $A^C_{UU} = \frac{d^5\sigma^+_{UU} - d^5\sigma^-_{UU}}{d^5\sigma^+_{UU} + d^5\sigma^-_{UU}}$.

DDVCS experimental observables

Considering the following asymmetries[a] both for JLab and EIC kinematics [b].

- $A_{LU} \propto \sin(\phi)\Im\left((F_1\mathcal{H} - kF_2\mathcal{E}) + \xi'(F_1+F_2)\tilde{\mathcal{H}}\right)$
- $A_{UU}^{C} \propto \cos(\phi)\Re\left(\frac{\xi'}{\xi}(F_1\mathcal{H} - kF_2\mathcal{E}) + \xi(F_1+F_2)\tilde{\mathcal{H}}\right)$
- $A_{UL} \propto \sin(\phi)\Im\left(F_1\tilde{\mathcal{H}} + \xi'(F_1+F_2)\left(\mathcal{H} + \frac{\xi}{1+\xi}\mathcal{E}\right) - \xi\left(\frac{\xi}{1+\xi}F_1 + kF_2\right)\tilde{\mathcal{E}}\right)$
- $A_{LL} \propto A + B\cos(\phi)$
  - $A \propto \Re\left(\xi(F_1+F_2)\left(\mathcal{H} + \frac{\xi}{1+\xi}\mathcal{E}\right) + F_1\tilde{\mathcal{H}} - \xi\left(\frac{\xi}{1+\xi}F_1 + kF_2\right)\tilde{\mathcal{E}}\right)$
  - $B \propto \Re\left(\xi(F_1+F_2)\left(\mathcal{H} + \frac{\xi}{1+\xi}\mathcal{E}\right) + \frac{\xi'}{\xi}F_1\tilde{\mathcal{H}} - \xi'\left(\frac{\xi}{1+\xi}F_1 + kF_2\right)\tilde{\mathcal{E}}\right)$

- A_{LU} and A_{UU}^{C} are GPD H dominated.
- A_{LU} and A_{LL} are GPD $\tilde{H}$ dominated.
- Due to the ξ' dependence, the coefficients in A_{LL} no longer have the same CFF dependence. Likewise for A_{LU} and A_{UU}^{C}.

[a] Considering the cross-section integrated over muon angles

[b] A. V. Belitsky et al. In: Physical Review D 68.11 (2003), p. 116005

Motivation

To model GPDs, the models used for evaluations are:

- VGG: Orsay's code [6–9].
- GK19: Latest model from PARTONS [10–12]
- KM10, KM15: Models from Gepard[a] [13, 14]
- AFKM12: KM model adaptation for EIC kinematics[b], also in Gepard.

The main goal of this study is to:

- Quantify the GPD dependence of the DDVCS observables within a reasonable kinematic window.
- Look for kinematic regions where models can be discriminated.
- Study the feasibility of the observable measurements considering JLab and EIC experimental configurations.

[a] Homemade adapted for DDVCS computations.

[b] E. Aschenauer et al. Journal of High Energy Physics 2013.9 (2013), pp. 1–59

Sensitivity @ JLab kinematics

It was studied in the LOI12-16-004 (S. Stepanyan et al.) the kinematic reach of DDVCS with CLAS12

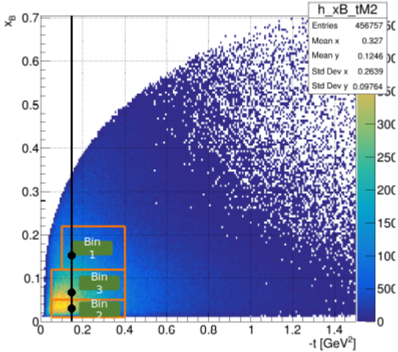

Figure: x_B vs t.

We perform a (Q^2, Q'^2) exploration at:

- $t = -0.15$ GeV^2.
- $x_B = 0.15, 0.07, 0.03$.

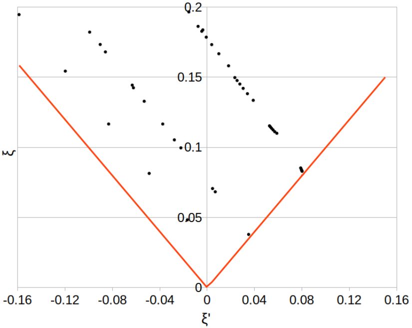

Figure: ξ vs ξ'

- Assuming $\mathcal{L} = 10^{37}$ cm^{-2} s^{-1}
- 5% of combined reconstruction and acceptance efficiency
- 100 days of beam time.

Sensitivity @ JLab kinematics

$x_B = 0.15,\ Q^2 = 2.77\ \mathrm{GeV}^2,\ Q'^2 = 1.0\ \mathrm{GeV}^2$

A_{LU} GPD H dominated A^C_{UU}

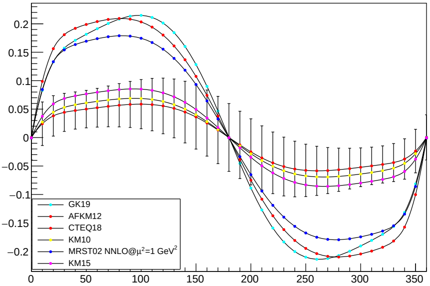

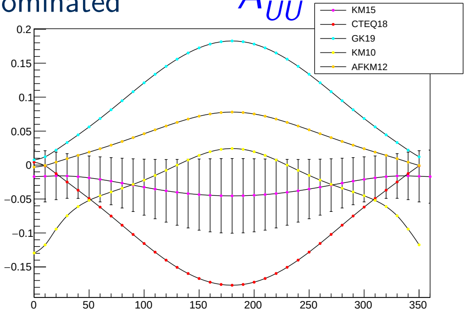

- ✓ Measurements are possible under 100 days of beam time.
- ✓ A_{LU} is sensitive to models. VGG & GK19 models vs KM ones.
- ✓ A^C_{UU} is sensitive to models. GK19 vs the others.
- ✓ VGG & KM15 models predict a different sign for A^C_{UU}.

Sensitivity @ JLab kinematics

$$x_B = 0.15,\ Q^2 = 2.77\ \mathrm{GeV}^2,\ Q'^2 = 1.0\ \mathrm{GeV}^2$$

A_{UL}

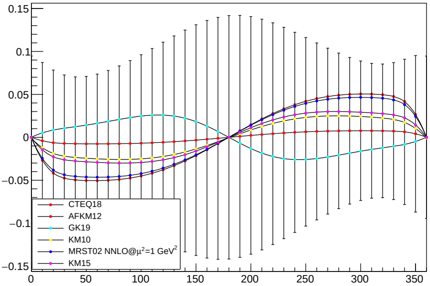

GPD $\tilde{H}$ dominated, sensitive to $\tilde{E}$.

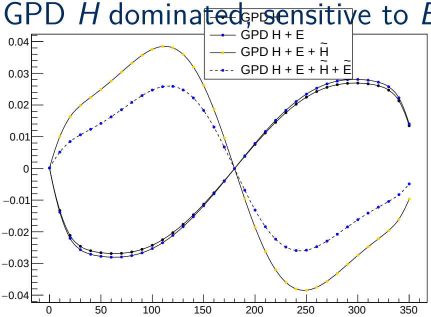

- ✗ Small amplitudes expected.
- ✗ Require more than 100 days of beam time.

Sensitivity @ JLab kinematics

$$x_B = 0.07,\ Q^2 = 0.8\ \text{GeV}^2,\ Q'^2 = 2.4\ \text{GeV}^2$$

A_{LL}

Sensitive to GPD H, $\tilde{H}$ and $\tilde{E}$

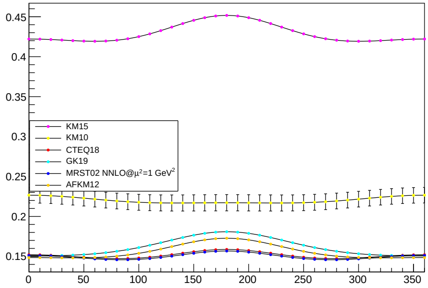

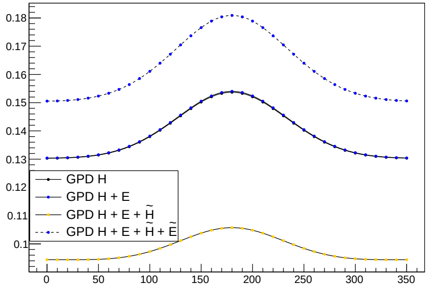

- ✓ Provides big asymmetry values.
- ✓ Measurable under 100 days with very good precision.
- ✗ Only not sensitive to GPD E.
- ✓ Sensitive to models. KM15 & KM10 vs the other models.

Sensitivity @ EIC kinematics

The cross-section drops quickly with Q'^2 [15, 16], then we explore on:

- $0.5 < Q^2(\mathrm{GeV}^2) < 3$, steps of 0.5
- $4m_\mu^2 < Q'^2(\mathrm{GeV}^2) < 3$,steps of 0.3
- $t = -0.15$ GeV^2.
- $x_B = 10^{-3}, 10^{-4}$.

- Assuming $\mathcal{L} = 10$ fb^{-1} year^{-1}
- 5% of combined reconstruction and acceptance efficiency
- 1 effective year of beam time.

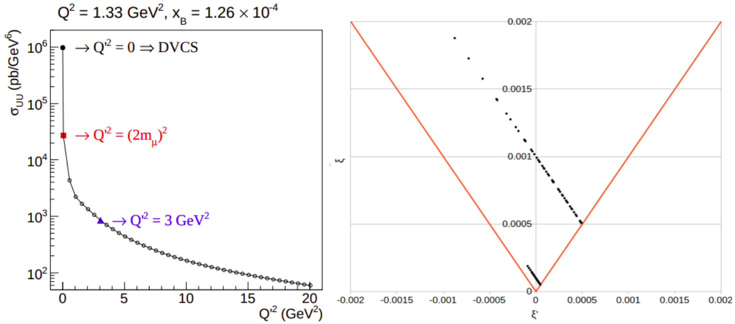

Figure: Left: unpolarized cross-section as a function of Q'^2. **Right:** ξ vs ξ' explored phase space. Smaller x_B regions corresponds to lines closer to the vertex.

Sensitivity @ EIC kinematics

As $x_B \to 0$, ξ, $\xi' \to 0$ as well. Then at LO in ξ and ξ' we get:

- $A_{LU} \propto \sin(\phi)\Im(\quad(F_1\mathcal{H} - kF_2\mathcal{E}))$
- $A_{UU}^{C} \propto \cos(\phi)\Re\left(\frac{\xi'}{\xi}(F_1\mathcal{H} - kF_2\mathcal{E})\right)$
- $A_{UL} \propto \sin(\phi)\Im\left(F_1\tilde{\mathcal{H}}\right)$
- $A_{LL} \propto A + B\cos(\phi)$
  - $A, B \propto \Re(F_1\tilde{\mathcal{H}})$

Consequences of such region kinematic reach are:

- ✓ Allows for cleaner measurements of GPD H and $\tilde{H}$.
- ✓ Main corrections come from GPD E
- ✗ We lose most of the GPD sensitivity.
- ✗ On the explored region, A_{UL} and A_{LL} amplitudes are bellow 1%.

Sensitivity @ EIC kinematics

$$x_B = 10^{-4},\ Q^2 = 1.5\ \text{GeV}^2,\ Q'^2 = 0.34\ \text{GeV}^2$$

A_{LU} GPD H dominated A^C_{UU}

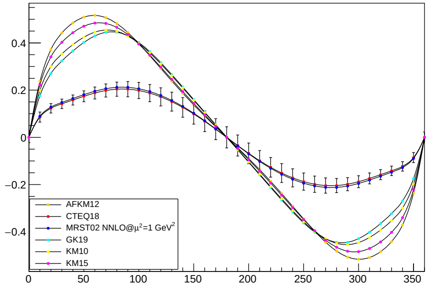

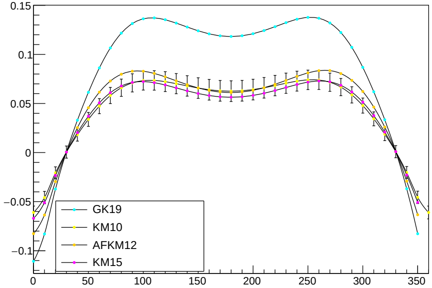

- ✓ Measurable within 1 year.
- ✓ The increase in the cross-section compensates the smaller luminosity, explaining the smaller error bars.
- ✓ A_{LU} sensitive to models. VGG vs the other models.
- ✓ A^C_{UU} sensitive to models. GK19 model vs the other models.

Sensitivity @ EIC kinematics

Furthermore, we can consider **transverse target asymmetries** which are mainly **sensitive to GPD** E.

$$A_{UT} \sim$$

$$+\cos(\Phi-\phi)\sin(\phi)\frac{2k}{1+\xi}\Re\left(\xi(F_1+F_2)\mathcal{E}-\frac{\xi'}{\xi}(F_2\tilde{\mathcal{H}}-\xi F_1\tilde{\mathcal{E}})\right)$$

$$+\sin(\Phi-\phi)\cos(\phi)\frac{2k}{1+\xi}\frac{\xi'}{\xi}\Im\left(F_2\mathcal{H}+F_1\mathcal{E}\right)$$

Here Φ is the azimuthal angle of the target polarization vector and we only keep terms up to linear order in ξ and ξ'.

Sensitivity @ EIC kinematics

$$x_B = 10^{-4},\ Q^2 = 1.5\ \text{GeV}^2,\ Q'^2 = 0.34\ \text{GeV}^2$$

A_{UT}

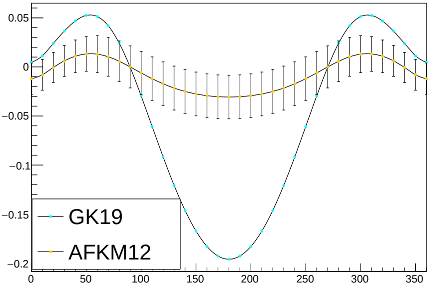

GPD E dominated

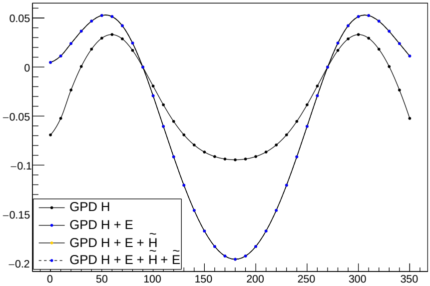

- ✓ Measurable within 1 year.
- ✓ Good opportunity to measure GPD E.
- ✓ Sensitive to models.

Conclusions

- The ξ' dependence of the DDVCS observables allow us to access more information about GPDs.
- At JLab kinematics:
  - Measurements of A_{LU}, A_{LL} and A_{UU}^{C} are sensitive to models.
  - Measurements of A_{UL} are not possible due to a large beam time requirement.
  - Measurements of A_{LL} can be done with more precision and separate further the KM15 and KM10 models from the others.
  - On A_{UU}^{C}, a sign change is predicted by KM15 & VGG models.
  - The above mentioned measurements can be achieved within 100 days of beam time.
- At EIC kinematics:
  - A_{LU} and A_{UU}^{C} are sensitive to models. Separating the VGG model and the GK19 model respectively.
  - In the explored kinematics, A_{UL} and A_{LL} have negligible amplitudes.
  - A_{UT} has a sizeable amplitude and is very sensitive on GPD E.
  - The above mentioned measurements can be achieved within 1 effective year of beam time.

References I

[1] E. Voutier et al. In: *Jefferson Lab Experiment LOI12-15-005* (2015).

[2] A. Accardi et al. In: *Eur. Phys. J. A* 57 (2021), p. 261.

[3] E. Voutier et al. In: *IPAC 13-The 4th International Particle Accelerator Conference*. Joint Accelerator Conferences Website. 2013, pp. 2088–2090.

[4] J. Grames et al. In: *arXiv preprint arXiv:2309.15581* (2023).

[5] A. Accardi et al. In: *The European Physical Journal A* 52 (2016), pp. 1–100.

[6] M. Vanderhaeghen et al. In: *Physical review letters* 80.23 (1998), p. 5064.

[7] M. Vanderhaeghen et al. In: *Physical Review D* 60.9 (1999), p. 094017.

References II

[8] K. Goeke et al. In: *Progress in Particle and Nuclear Physics* 47.2 (2001), pp. 401–515.

[9] M. Guidal et al. In: *Physical Review D* 72.5 (2005), p. 054013.

[10] S. Goloskokov et al. In: *The European Physical Journal C* 50 (2007), pp. 829–842.

[11] S. Goloskokov and P. Kroll. In: *The European Physical Journal C* 53 (2008), pp. 367–384.

[12] B. Berthou et al. In: *Eur. Phys. J. C* 78.6 (2018), p. 478. DOI: 10.1140/epjc/s10052-018-5948-0. arXiv: 1512.06174 [hep-ph].

[13] K. Kumerički and D. Mueller. In: *Nuclear Physics B* 841.1-2 (2010), pp. 1–58.

References III

[14] K. Kumerički. *Gepard: Tool for studying the 3d quark and gluon distributions in the nucleon*. https://gepard.phy.hr/credits.html.

[15] S. Y. Zhao. "Access to decoupled information of Generalized Parton Distributions via Double Deeply Virtual Compton Scattering". HADRON 2019. 2019. URL: %5Curl%7Bhttps://indico.ihep.ac.cn/event/9119/contributions/107033/attachments/57434/66243/HADRON_Shengying_ZHAO.pdf%7D.

[16] Shengying Zhao. "Access to decoupled information on Generalized Parton Distributions (GPDs) via Double Deeply Virtual Compton Scattering (DDVCS)". In: *HADRON SPECTROSCOPY AND STRUCTURE: Proceedings of the XVIII International Conference*. World Scientific. 2021, pp. 592–596.

Thanks

Thanks

Backup

Backup

DDVCS experimental observables

- DDVCS interferes with two kind of BH processes.
  - Interference term is accessible through asymmetries.

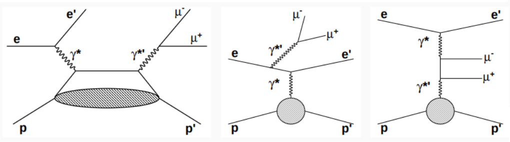

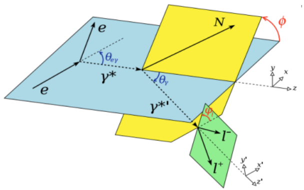

$$\sigma \propto \mathcal{T}^2 = |\mathcal{T}_{\text{ddvcs}}|^2 + |\mathcal{T}_{\text{BH}_1} + \mathcal{T}_{\text{BH}_2}|^2 + \mathcal{I} \text{ (linear in Compton form factors)}$$

Exclusive leptoproduction reactions

Two golden channels for GPD measurements are **DVCS** and **DDVCS**.

$ep \to ep\gamma$

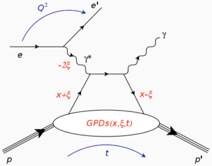

Deeply Virtual Compton Scattering (DVCS)

$$\mathcal{H}(\xi,\xi,t)=\sum_q e_q^2\Big\{\mathcal{P}\int_{-1}^{1}dx\, H^q(x,\xi,t)\left[\frac{1}{x-\xi}+\frac{1}{x+\xi}\right] - i\pi\left[H^q(\xi,\xi,t)-H^q(-\xi,\xi,t)\right]\Big\}$$

$ep \to epl^- l^+$

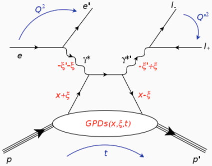

Double DVCS (DDVCS)

$$\mathcal{H}(\xi',\xi,t)=\sum_q e_q^2\Big\{\mathcal{P}\int_{-1}^{1}dx\, H^q(x,\xi,t)\left[\frac{1}{x-\xi'}+\frac{1}{x+\xi'}\right] - i\pi\left[H^q(\xi',\xi,t)-H^q(-\xi',\xi,t)\right]\Big\}$$

- DVCS access GPDs at $x=\pm\xi$
- DDVCS access GPDs at independent $x=\xi'$ and ξ values ($|\xi'|<\xi$).

$$\xi'=\frac{Q^2-Q'^2+t/2}{2Q^2/x_B-Q^2-Q'^2+t}$$

$$\xi=\frac{Q^2+Q'^2}{2Q^2/x_B-Q^2-Q'^2+t}$$

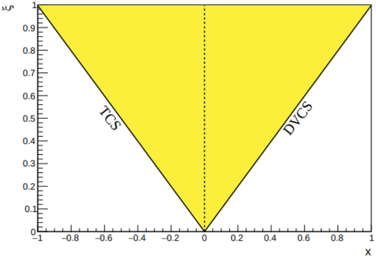

Sensitivity @ EIC kinematics

- As $W = 140$ GeV, the equivalent beam energy is $E \approx \frac{W^2}{2M} \approx 9800$ GeV.
  - At EIC kinematics, the DDVCS cross section increases importantly.
  - The cross section increase compensates the smaller luminosity.

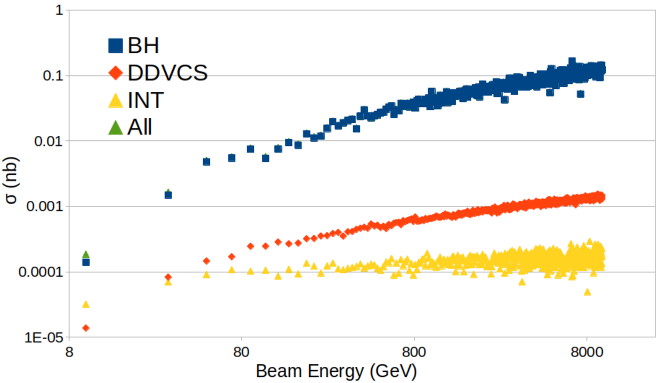

Figure: Integrated cross section from JLab to EIC kinematics. Obtained with PARTONS [12].

General scan JLab

$x_B = 0.15$

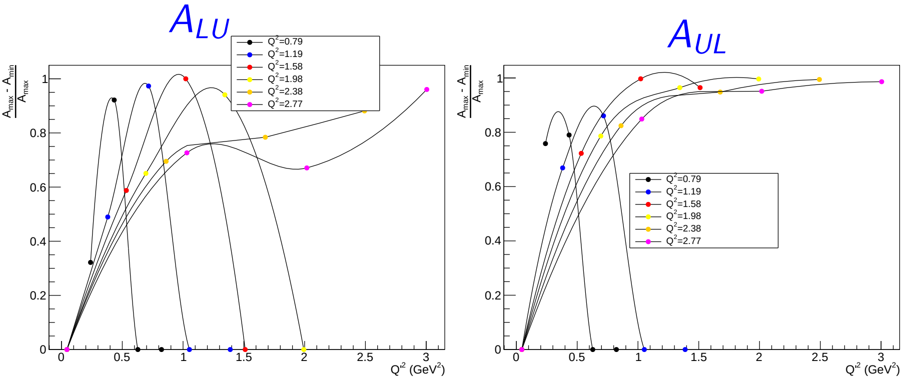

$\frac{A_{max}-A_{min}}{A_{max}}$ over models on the general scan. Only points with amplitudes greater than 1% are considered.

General scan JLab

$$x_B = 0.15$$

A_{LL} A_{UU}^C

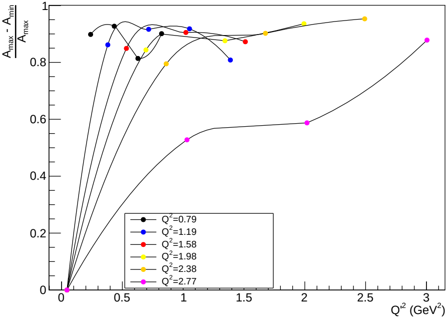

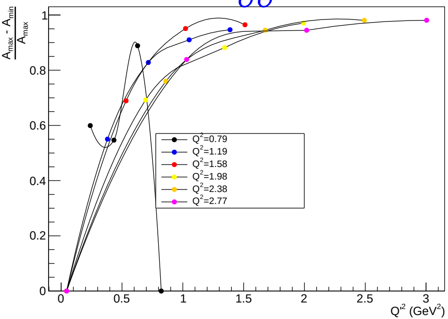

$\frac{A_{max}-A_{min}}{A_{max}}$ over models on the general scan. Only points with amplitudes greater than 1% are considered.

General scan JLab

$x_B = 0.03$

A_{LU}

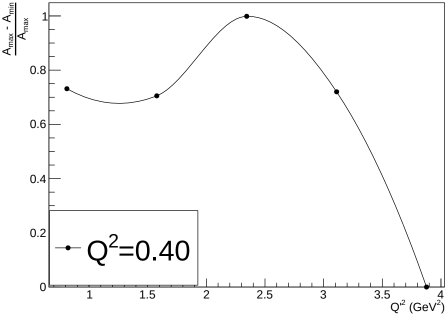

A_{UL}

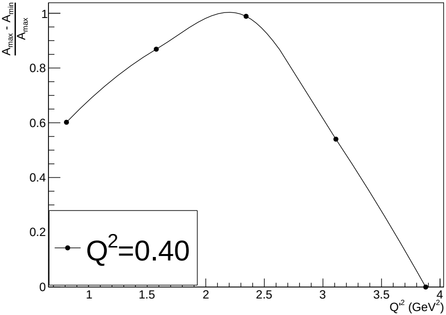

$\frac{A_{max}-A_{min}}{A_{max}}$ over models on the general scan. Only points with amplitudes greater than 1% are considered.

General scan JLab

$$x_B = 0.03$$

A_{LL}

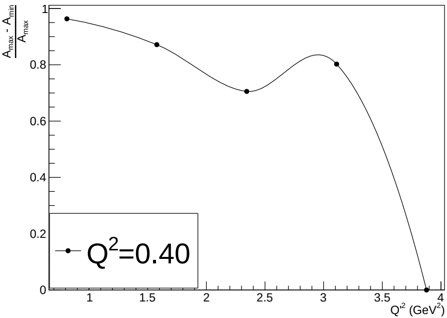

A_{UU}^{C}

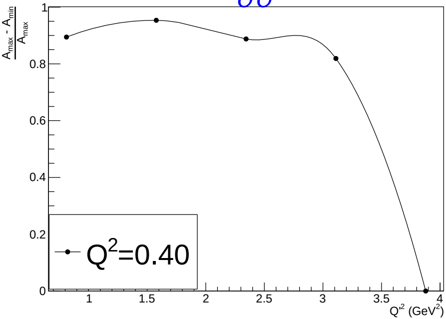

$\frac{A_{max}-A_{min}}{A_{max}}$ over models on the general scan. Only points with amplitudes greater than 1% are considered.

General scan JLab

$x_B = 0.07$

A_{LU}

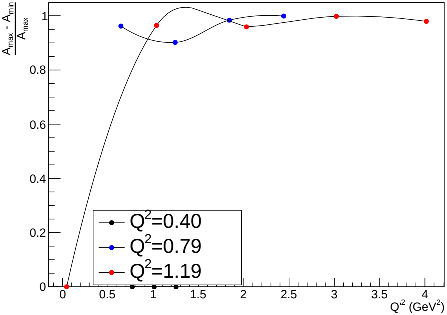

A_{UL}

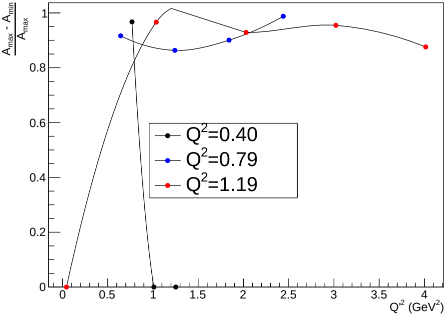

$\frac{A_{max}-A_{min}}{A_{max}}$ over models on the general scan. Only points with amplitudes greater than 1% are considered.

General scan JLab

$x_B = 0.07$

A_{LL}

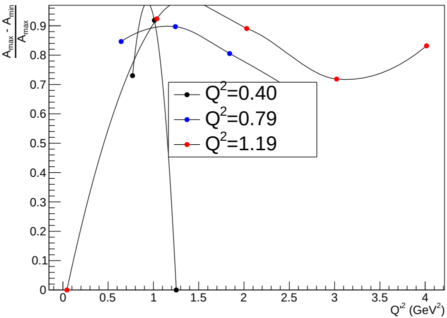

A^C_{UU}

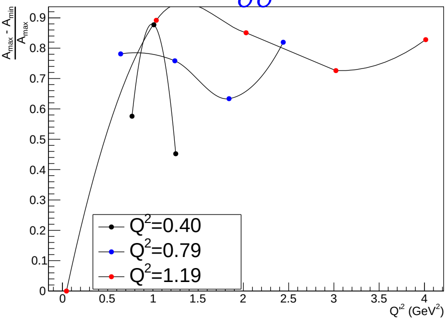

$\frac{A_{max}-A_{min}}{A_{max}}$ over models on the general scan. Only points with amplitudes greater than 1% are considered.

General scan EIC

$$x_B = 10^{-3}$$

A_{LU}

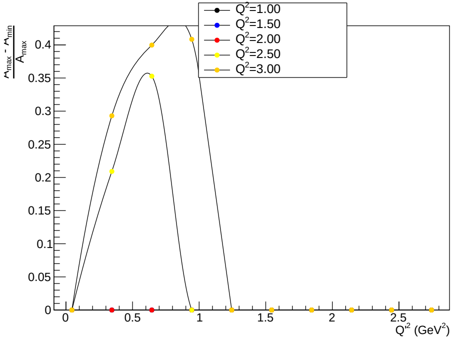

A^C_{UU}

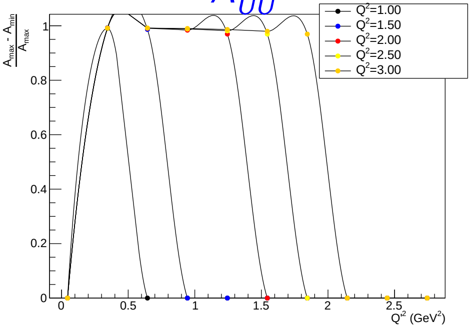

$\frac{A_{max}-A_{min}}{A_{max}}$ over models on the general scan. Only points with amplitudes greater than 1% are considered.

General scan EIC

$$x_B = 10^{-4}$$

A_{LU}

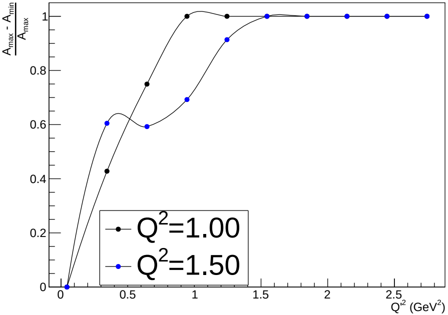

A^C_{UU}

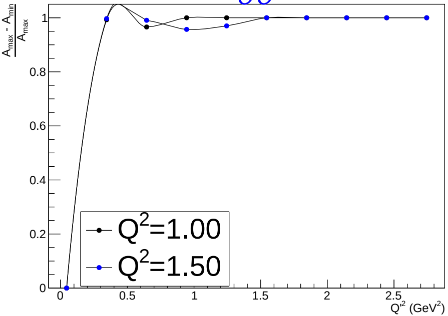

$\frac{A_{max}-A_{min}}{A_{max}}$ over models on the general scan. Only points with amplitudes greater than 1% are considered.

General scan EIC

A_{UT}

$x_B = 10^{-3}$

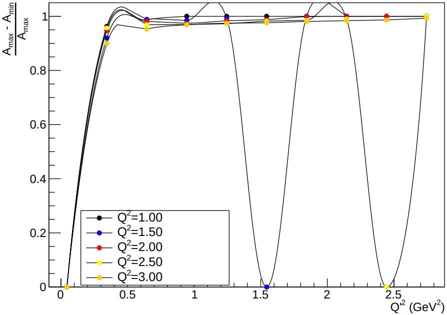

$x_B = 10^{-4}$

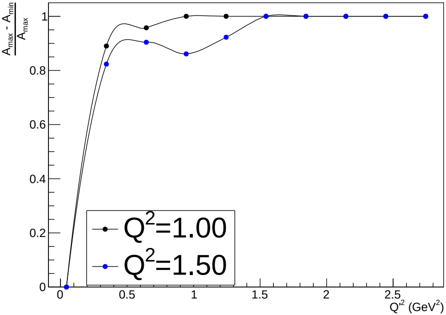

$\frac{A_{max}-A_{min}}{A_{max}}$ over models on the general scan. Only points with amplitudes greater than 1% are considered.

Backup: Gepard modifications

- For CFF $\mathcal{H}$, the dispersion relation is based on the imaginary part.
  - For DVCS: $H(x,x,t) = \frac{nr}{1+x}\left(\frac{2x}{1+x}\right)^{-\alpha(t)}\left(\frac{1-x}{1+x}\right)^{b}\frac{1}{\left(1-\frac{1-x}{1+x}\frac{t}{M^2}\right)^{p}}.$
  - For DDVCS, an inverse ingineering was done to find a DD that reproduces the DVCS case, then it was generalized $H(x,\xi,t) =$ $\frac{nr\vartheta}{\vartheta+x}\frac{1+\vartheta}{2}\left(\frac{(1+\vartheta)x}{\vartheta+x}\right)^{-\alpha(t)}\left(\frac{\vartheta^2(1+\vartheta)}{2}\frac{1-x}{\vartheta+x}\right)^{b}\frac{1}{\left(1-(1-\vartheta^2)\frac{t}{M^2}-\frac{\vartheta^2(1+\vartheta)}{2}\frac{(1-x)}{\vartheta+x}\frac{t}{M^2}\right)^{p}}$

  being $\vartheta = x/\xi$. Notice that for $\vartheta = 1$ reproduces the DVCS case.

Backup: Gepard modifications

- Likewise for CFF $\tilde{\mathcal{H}} = \pi \left(2\frac{4}{9} + \frac{1}{9}\right)$
  $\frac{\tilde{n}\vartheta}{\vartheta+x} \frac{1+\vartheta}{2} \left(\frac{(1+\vartheta)x}{\vartheta+x}\right)^{-\alpha(t)} \left(\frac{\vartheta^2(1+\vartheta)}{2} \frac{1-x}{\vartheta+x}\right)^{3/2} \frac{1}{1-(1-\vartheta^2)\frac{t}{M^2} - \frac{\vartheta^2(1+\vartheta)(1-x)}{\vartheta+x} \frac{t}{2M^2}}$
- For CFF $\mathcal{E}$ there is no implementation for a dispersion relation.
- for CFF $\tilde{\mathcal{E}}$ we can perform exact computations:
  - $\int_{-1}^{1} dx \left[\frac{1}{x-\xi+i\epsilon} - \frac{1}{x+\xi-i\epsilon}\right] \tilde{E}(x,\xi,t) = -\frac{1}{2\xi} h_A(t)$
  - $\int_{-1}^{1} dx \left[\frac{1}{x-\xi'+i\epsilon} - \frac{1}{x+\xi'-i\epsilon}\right] \tilde{E}(x,\xi,t) =$
    $-\frac{1}{8\xi^3} h_A(t) \left(4\xi\xi' + 2(\xi^2 - \xi'^2) \log\left(\frac{\xi+\xi'}{\xi-\xi'}\right)\right)$

Backup: Remarks

- KM Im(H) and Im(Ht) parametrization are not odd functions as required, so I force that condition by mirroring the x>0 region.
- AFKM12 only has GPD H and E
- For regular KM models Im(E)=Im(Et)=0
- In VGG, GPD E DD is chosen with a factorized t anzats (option 4)